

Two-proton capture on the ^{68}Se nucleus with a new self-consistent cluster model

D. Hove^a, E. Garrido^b, A.S. Jensen^a, P. Sarriguren^b, H.O.U. Fynbo^a, D.V. Fedorov^a, N.T. Zinner^a

^a*Department of Physics and Astronomy, Aarhus University, DK-8000 Aarhus C, Denmark*

^b*Instituto de Estructura de la Materia, IEM-CSIC, Serrano 123, E-28042 Madrid, Spain*

Abstract

We investigate the two-proton capture reaction of the prominent rapid proton capture waiting point nucleus, ^{68}Se , that produces the borromean nucleus ^{70}Kr ($^{68}\text{Se}+p+p$). We apply a recently formulated general model where the core nucleus, ^{68}Se , is treated in the mean-field approximation and the three-body problem of the two valence protons and the core is solved exactly. The same Skyrme interaction is used to find core-nucleon and core valence-proton interactions. We calculate $E2$ electromagnetic two-proton dissociation and capture cross sections, and derive the temperature dependent capture rates. We vary the unknown 2^+ resonance energy without changing any of the structures computed self-consistently for both core and valence particles. We find rates increasing quickly with temperature below 2 – 4 GK after which we find rates varying by less than a factor of two independent of 2^+ resonance energy. The capture mechanism is sequential through the $f_{5/2}$ proton-core resonance, but the continuum background contributes significantly.

Keywords: rp-process, capture rate, electric dissociation, three-body, mean-field

PACS: 25.40.Lw, 26.30.Hj, 21.45.-v, 21.60.Jz

1. Introduction

The abundance of most stable nuclei above iron in the universe can be understood as produced by various types of neutron capture [1, 2]. However, production of about 40 stable isotopes cannot be explained in this way, but only through similar proton capture processes [3, 4, 5, 6, 7]. The basic ignition fuel is a large proton flux arising from a stellar explosion. The sequence of these reactions are then one proton capture after another until the proton dripline is reached and further captured protons are immediately emitted. This dripline nucleus usually must wait to beta-decay to a more stable nucleus which in turn can capture protons anew. This is the "rp-process" [8, 9]. These p-nuclei are also believed to be produced by other methods: gamma-proton [4, 10] and neutrino-proton processes [11, 12].

The beta-decay waiting time is large for some of these nuclei along the dripline, which for that reason are denoted waiting points [13]. However, another path is possible to follow for borromean proton dripline nuclei where two protons, in contrast to one, are necessary to produce a bound nucleus. Then two protons can be captured before beta-decay occurs [14, 15]. The capture

time and the corresponding mechanism are therefore important for the description of the outcome of these astrophysical processes [16, 17].

We focus in this letter on one of these two-proton capture reactions leading from a prominent waiting point nucleus, ^{68}Se [18, 19], to formation of the borromean proton dripline nucleus, ^{70}Kr ($^{68}\text{Se}+p+p$). The specific experimental reaction information is not available, and theoretical estimates are, at least at the moment, unavoidable [20, 21, 22].

Traditionally, the reactions have been described as sequential one-proton capture by tunneling through the combined Coulomb plus centrifugal barrier. The tunneling capture mechanisms have been discussed as direct, sequential and virtual sequential decay [23, 24, 25, 26]. They are all accounted for in the present formulation. The capture rate depends on temperature through the assumed Maxwell-Boltzmann energy distribution. It is then important to know the energy dependence of the capture cross section for given resonance energies, and especially in the Gamow window [27].

Clearly the desired detailed description requires a three-body model which is available and even applied to the present processes [28, 29]. However, the crucial proton-core potentials have so-far been chosen phe-

Email address: dennish@phys.au.dk (D. Hove)

nomenologically to produce the essentially unknown, but crucial, single-particle energies. A new model involving both core and valence degrees of freedom was recently constructed to provide mean-field proton potentials derived from the effective nucleon-nucleon mean-field interaction [30, 31, 32]. In turn these potentials produce new and different effective three-body potentials, which in the present letter is exploited to investigate the two-proton capture rates.

The techniques are in place all the way from the solution of the coupled core and valence proton system [28, 31, 32], over the self-consistent three-body input and subsequent calculations [33, 34], to the capture cross sections and rates [35, 36, 37, 38]. We shall first sketch the steps in the procedure used in the calculations. Then we shall discuss in more details the numerical results of interest for the astrophysical network computations, which calculates the abundances of the isotopes in the Universe.

2. Theoretical description

The basic formulation and the procedure are described in [28, 35, 39]. The framework is the three-body technique but based on the proton-core potential derived through the self-consistently solved coupled core-plus-valence-protons equations [30, 31]. The procedure is first to select the three-body method, second to formulate how to calculate the capture rate, and finally to choose the numerical parameters to be used in the computations.

2.1. Wave functions

First, the many-body problem is solved for a mean-field treated core interacting with two surrounding valence protons [28]. The details of this recent model are very elaborate, but already applied on two different neutron dripline nuclei [28, 30]. It then suffices to sketch the corresponding details for the present application. Briefly, the novel features are to find the mean-field solution for the core-nucleons in the presence of the external field from the two valence protons. In turn, folding the basic nucleon-nucleon interaction and the core wave function provides the interaction between each valence proton and the core nucleus. The interactions between core and valence nucleons then depend on their respective wave functions, which are found self-consistently by iteration. We emphasize that the same nucleon-nucleon interaction is used both in the core and for this valence-proton core calculation. The crucial main ingredient in the three-body solution is this interaction,

which then is provided by the procedure and determined independent of subsequent applications.

The present application exploits the properties of the derived three-body solution. The three-body problem is solved by adiabatic expansion of the Faddeev equations [29] in hyperspherical coordinates. When necessary the continuum is discretized by a large box confinement [40]. The main coordinate is the hyperradius, ρ , defined as the mean radial coordinate in the three-body system [39, 41]. More specifically we have

$$(2m_n + m_c)\rho^2 = m_n(\mathbf{r}_{v_1} - \mathbf{r}_{v_2})^2 + m_c \sum_{i=1}^2 (\mathbf{r}_{v_i} - \mathbf{R}_c)^2 \quad (1)$$

where m_n , m_c , \mathbf{r}_{v_1} , \mathbf{r}_{v_2} and \mathbf{R}_c are neutron mass, core mass, valence-proton coordinates and core center-of-mass coordinate, respectively. The three-body wave function is found through this procedure for given angular momenta as functions of the hyperspherical coordinates for the required ground state (Ψ_J). When necessary the continuum is discretized by a large box confinement and the discretized continuum states ($\psi_j^{(i)}$) are calculated.

2.2. Reactions

The two-proton capture reaction $p + p + c \leftrightarrow A + \gamma$ cross section σ_{ppc} and the photodissociation cross section σ_γ^λ of order λ are related [39]. The three-body energy, E , and the ground state energy, E_{gr} , determine the photon energy by $E_\gamma = E + |E_{gr}|$. The dissociation cross section is then given by

$$\sigma_\gamma^\lambda(E_\gamma) = \frac{(2\pi)^3(\lambda+1)}{\lambda((2\lambda+1)!!)^2} \left(\frac{E_\gamma}{\hbar c}\right)^{2\lambda-1} \frac{d}{dE} \mathcal{B}(E\lambda, 0 \rightarrow \lambda), \quad (2)$$

where the strength function for the $E\lambda$ transition,

$$\frac{d}{dE} \mathcal{B}(E\lambda, 0 \rightarrow \lambda) = \sum_i |\langle \psi_\lambda^{(i)} | \hat{\Theta}_\lambda | \Psi_0 \rangle|^2 \delta(E - E_i), \quad (3)$$

is given by the reduced matrix elements, $\langle \psi_\lambda^{(i)} | \hat{\Theta}_\lambda | \Psi_0 \rangle$, where $\hat{\Theta}_\lambda$ is the electric multipole operator, $\psi_\lambda^{(i)}$ is the wave function of energy, E_i , for all bound and (discretized) three-body continuum states in the summation. The capture reaction rate, R_{ppc} , is given by Ref. [37]

$$R_{ppc}(E) = \frac{8\pi}{(\mu_{cp}\mu_{cp,p})^{3/2}} \frac{\hbar^3}{c^2} \left(\frac{E_\gamma}{E}\right)^2 \sigma_\gamma^\lambda(E_\gamma), \quad (4)$$

where μ_{cp} and $\mu_{cp,p}$ are reduced masses of proton and core and proton-plus-core and proton, respectively. For

the astrophysical processes in a gas of temperature, T , we have to average the rate in Eq. (4) over the corresponding Maxwell-Boltzmann distribution, $B(E, T) = \frac{1}{2} E^2 \exp(-E/T)/T^3$,

$$\langle R_{ppc}(E) \rangle = \frac{1}{2T^3} \int E^2 R_{ppc}(E) \exp(-E/T) dE, \quad (5)$$

where the temperature is in units of energy.

2.3. Interactions

The decisive interaction is first of all related to the mean-field calculation of the core. We use the Skyrme interaction SLy4 [42] with acceptable global average properties. The application on one specific nuclear system requires some adjustment to provide the known borromean character, that is unbound proton-core $f_{5/2}$ resonance at 0.6 MeV [43] and two protons bound to the core. With a minimum of changes we achieve this by shifting all energies while leaving the established structure almost completely unaltered. The simplest consistent such modification is by scaling all the main Skyrme strength parameters, t_i , by the same factor, 0.9515.

The density dependence of the Skyrme interaction can be viewed as a parametrized three-body potential. To simulate that effect we employ a short-range Gaussian, $S_0 \exp(-\rho^2/b^2)$, which depends on the three-body hyperradial coordinate ρ . We choose $b = 6$ fm and leave S_0 to fine-tune each of the 0^+ and 2^+ three-body energies. This is necessary since the keV-scale of binding is crucial for tunneling through single MeV height barriers. This level of accuracy is beyond the present capability of many-body model calculations. To reproduce the predicted 0^+ energy of -1.34 MeV [44] a three-body strength $S_0 = -17.5$ MeV is needed. The unknown 2^+ energy is varied from almost bound, zero energy, to the top of the barrier by S_0 changing from -35.05 MeV to -26.22 MeV.

3. Effective three-body potentials

The elaborate numerical calculations produce the sets of coupled “one-body” effective potentials depending on hyperradius as shown in Fig. 1 for both 0^+ and 2^+ . The continuations beyond the 20 fm in the figure are almost quantitatively Coulomb plus centrifugal behavior and as such reveal no surprises. The kinks and fast bends reflect avoided crossings and related structure changes. They are especially abundant at small distances and around the barriers. The diagonal non-adiabatic coupling terms as well as the diagonal structure-less three-body Gaussian potentials are included in the calculations, but not in the figure. They

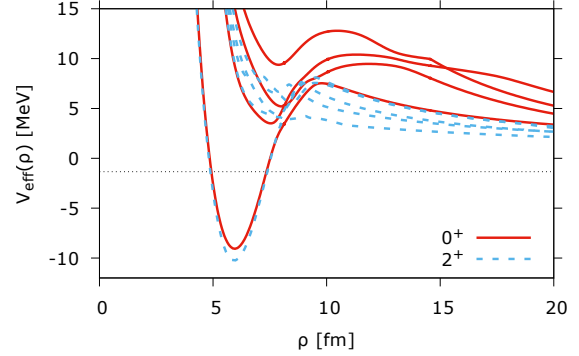


Figure 1: The effective, adiabatic potentials for the 0^+ (red, solid), and the 2^+ (light-blue, dashed) configuration in $^{68}\text{Se} + p + p$ using the SLy4 Skyrme interaction between core and valence protons, scaled to reproduce the experimental $f_{5/2}$ resonance energy of 0.6 MeV in $^{68}\text{Se} + p$ [43]. The dotted horizontal line is the 0^+ energy at -1.34 MeV from $S_0 = -17.5$ MeV.

both leave the structure essentially unaltered although they may change the energies of the solutions rather substantially.

The 0^+ ground-state at -1.34 MeV, predicted from systematics [45], is reproduced with the chosen parameters. The structure corresponds to the configuration of the pronounced minimum in the lowest 0^+ potential. No 0^+ resonance are produced by the potentials in Fig. 1. The ground state is the final state in the capture process independent of the specific mechanism.

However, the decisive capture process proceeds within the 2^+ continuum from the large to the short-distance attractive region of the potentials shown in Fig. 1. This lowest minimum is rather similar to the 0^+ minimum but the non-adiabatic repulsive terms increase the energy substantially. Unfortunately nothing is known about a 2^+ resonance which would strongly influence the capture rate. Consequently the strength, S_0 , is used to vary the position of the 2^+ resonance from almost bound to disappearance above the barriers. Both the resonance energy, the height, and the rather broad Coulomb shape of the barrier strongly influence the capture process.

The structure of these potentials is substantially simpler than those obtained in [28] where low-lying single-proton states $p_{3/2}$ and $f_{5/2}$ both appeared. The present simplification is an automatic result of the procedure using the nucleon-nucleon mean-field effective interaction to calculate the proton-core potential. This is not an ad hoc assumption, but arises naturally due to identical interactions for both core and valence particles. As such it is a novel deduction embedded in the design of our model. The lack of single-particle states of differ-

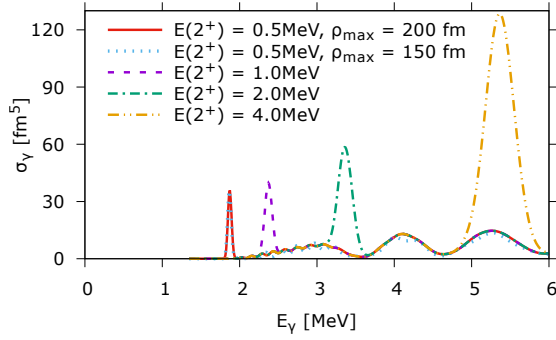


Figure 2: The electromagnetic $E2$ dissociation cross section, $\sigma_{\gamma}^{(l=2)}(E_{\gamma})$, for the process, $^{70}\text{Kr} + \gamma \rightarrow ^{68}\text{Se} + p + p$, as a function of photon energy. The 0^+ final state energy is -1.34 MeV and the 2^+ resonance energies are $E = 0.5, 1.0, 2.0$, and 4.0 MeV, respectively. The discretized continuum states are obtained using box sizes of $\rho_{\text{max}} = 150, 200$ fm.

ent parity implies that no 1^- three-body resonance states appear in the low-energy region. The transition is then necessarily an $E2$ transition, which contributes to the longer effective lifetime of the system, and could very well be part of the reason this system is a critical waiting point.

4. Quantitative results

The all-important core-valence proton potential is derived naturally and unambiguously by our mean-field core treatment, as discussed in the previous sections. As a result the two-proton capture cross section follows directly, only depending on the three-body resonance level. This is discussed in the following section, after which the resulting temperature averaged reaction rates are presented. This is supplemented by a discussion of the reaction mechanism and its implication for the possible reactions.

4.1. Cross section

The incident flux of low-energy protons on the core nucleus may result in capture. The corresponding cross section is most easily obtained from calculation of the inverse reaction, that is photodissociation of the 0^+ ground state, Ψ_0 , of ^{70}Kr . The discretized continuum states, $\psi_{\lambda}^{(i)}$, are computed and the cross section is obtained from Eqs. (3) and (2) with $\lambda = 2$. The two-proton capture cross section of ^{68}Se , obtained from Eq. (2), is shown in Fig. 2 as function of the three-body energy.

The peaks in the capture cross section occur at experimentally unknown resonance energies where the tunneling probability is large. We therefore vary the energy from 0.5 MeV to 4.0 MeV where the widths of the

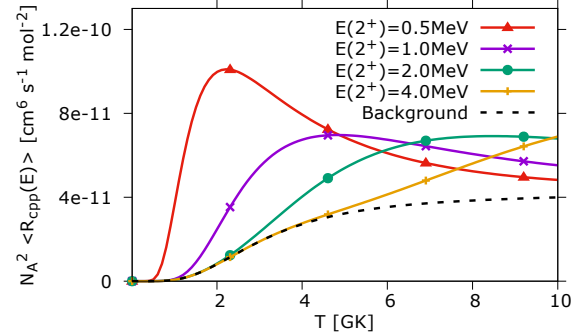


Figure 3: The reaction rate for the radiative capture process $^{68}\text{Se} + p + p \rightarrow ^{70}\text{Kr} + \gamma$, as function of temperature for the different 2^+ resonance energies in Fig. 2. The black dashed curve is the background contribution.

peaks in the cross section increase with energy as the top of the barrier is approached. We emphasize that the crucial quantity is the resonance energy. This can be tested by varying the number of adiabatic potentials used in the calculation. This results in somewhat different resonance energy which however can be compensated for by use of the three-body potential, which in turn recover the cross section in Fig. 2.

These features are simply understood as enhanced spatial overlaps between the 2^+ continuum states in the resonance region and the ground state wave function, expressed through Eq. (3). Besides the resonance contributions we also find significant, although several orders of magnitude smaller, background contributions, which incidentally is independent of the size of the discretization box, as long as it is sufficiently large [40].

4.2. Capture rates

The capture cross sections are the main ingredient in the calculation of the two-proton absorption rate appropriate for the temperature dependent astrophysical network computation. The average rate in Eq. (5) are shown in Fig. 3 as function of temperature. The Boltzmann smearing factor produces very smooth curves of the same qualitative behavior. They are zero at zero temperature and energy, because the barrier is infinitely thick. All rates then increase to a maximum at the Gamow peak where the best compromise is reached between the decreasing temperature distribution and the increasing tunneling probability.

The peak contribution moves to higher energy and becomes smoother with increasing resonance energy. Above temperatures of a few GK the average rate variation is moderate and the size roughly of order $\simeq 6 \times 10^{-11} \text{ cm}^6 [N_A \text{ mol}]^{-2} \text{ s}^{-1}$. A low-lying resonance energy

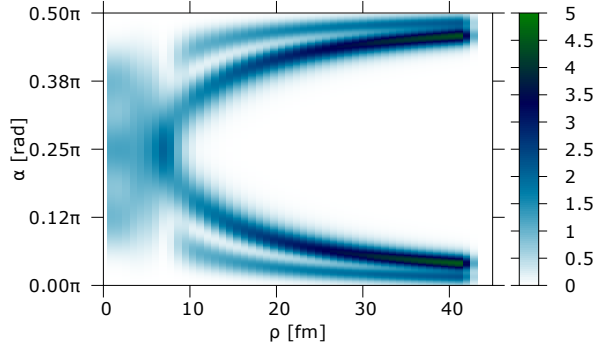


Figure 4: The probability of the three-body, $^{68}\text{Se} + p + p$, wave function for the lowest allowed potential, integrated over directional angles ($\sin^2(\alpha) \cos^2(\alpha) \int |\Phi_n(\alpha, \rho, \Omega_x, \Omega_y)|^2 d\Omega_x d\Omega_y$), as a function of hyperradius, ρ , and hyperangle, α , related to the Jacobi coordinate system where "x" is between core and proton.

corresponds to low-lying peak position of larger height. We emphasize that the background without resonance contribution obviously is smaller but only by roughly a factor of two as soon as the temperature exceeds about 4 GK (~ 0.34 MeV). In other words, if temperatures are in the astrophysically interesting range below about 1 GK, the size variations are substantial, and vice versa above a few GK the details from the microscopic origin are smeared out.

The actual size of the rate may reveal deceptively little variation at the relatively high temperatures. However, the barrier height and width are all-decisive and both may easily be different for other systems where the single-particle structure at the Fermi energy is different and perhaps more complicated as studied in [28]. The relatively large 2^+ background contribution might suggest significant corresponding 0^+ continuum contributions. However, the 0^+ barriers in Fig. 1 are larger and the $0^+ \rightarrow 0^+$ transition as well require processes involving atomic electrons. It is again worth emphasizing that a superficially more complete calculation with for example many coupled potentials would provide the same rates after adjusting to the same resonance energy.

4.3. Reaction mechanism

The rate depends on the capture mechanism. We are here only concerned with three-body capture, but a dense environment would enhance four-body capture processes as discussed in [36]. The overall three-body process is tunneling through a barrier of particles in a temperature distribution of given density. Once inside the relatively thick barrier they have essentially only the option of emitting photons to reach the bound ground-state. However, the first of this two-step process can oc-

cur through different mechanisms, where the most obvious possibility is to be captured in different angular momentum states. The conservation of angular momentum and parity quantum numbers are crucial in connection with resonance positions. If low-lying 1^- continuum states are allowed they would be preferred, and vice versa if prohibited 2^+ continuum states would be preferred. Low-lying resonances enhance the contributions substantially. This selection depends strongly on the nucleus under investigation.

For a given angular momentum of the three-body continuum states, we still may encounter several qualitatively different ways of absorbing two protons from the continuum [46]. These mechanisms were discussed in [23] for the inverse process of dissociation, that is direct, sequential and virtual sequential decay. They are all accounted for in the present formulation. In [28] we concluded that the direct process is most probable for very low three-body energy when two-body subsystems are unbound. If the energy is larger than stable two-body substructures such intermediate vehicles enhance the rates and the mechanism is sequential.

Even when it is energetically forbidden to populate two-body resonance states it may be advantageous to exploit these structures virtually while tunneling through an also energetically forbidden barrier. This is appropriately named the virtual sequential two-body mechanism. It may be appropriate to emphasize that a similar three-body virtual mechanism is forbidden because the three-body energy is conserved in contrast to the energy of any two-body subsystem.

The mechanism for the present capture process is revealed in Fig. 4 where the 2^+ probability integrated over the directional angles is shown for the lowest potential as function of hyperradius and one of the Jacobi angles. It is a strikingly simple structure for hyperradii larger than about 15 fm, which for these coordinates is equivalent to one proton at that distance from the center of mass of the combined proton-core system. Since the Jacobi angle, α , is either close to zero or $\pi/2$, this simply means that one proton is staying very close to the core for all these hyperradii. Eventually also this proton has to move away from the core since no bound state exist. But the process is sequential through this substructure which can be determined to be the proton-core $f_{5/2}$ resonance.

The higher-lying configurations corresponding to the three following potentials also show precisely the same $f_{5/2}$ structure. This is explained by combining the compact proton-core $f_{5/2}$ resonance with one non-interacting (apart from Coulomb and centrifugal) distant proton in any angular momentum configuration

consistent with a 2^+ structure. The angular momenta capable of combining with $f_{5/2}$ to produce 2^+ are $p_{1/2}$, $p_{3/2}$, $f_{5/2}$, $f_{7/2}$, and $h_{9/2}$. This also implies that for temperatures much smaller than the $f_{5/2}$ resonance energy it would be energetically advantageous to start the capture process in a configuration corresponding to direct three-body capture. The change of structure, around avoided level crossings, to two-body resonance configurations would then greatly reduce the barrier and substantially enhance the capture rate.

5. Conclusion

The new model that treats the core and the two valence particles self-consistently and simultaneously is applied on the waiting point nucleus (^{68}Se) for the astrophysical rp-process. This is done essentially without any free parameters or phenomenological fitting, which makes the results much less arbitrary than usual three-body calculations. Adding two protons, but not one, produces a bound system, ^{70}Kr , which is then a borromean nucleus. A moderate overall scaling of the Skyrme interaction SLy4 reproduces the scarcely known properties of these dripline nuclei. Other Skyrme interactions provide very similar results.

We calculate the radiative two-proton capture rate as function of temperature for different resonance energies. We investigate the mechanism and find that sequential capture of one proton after the other by far is dominating. The first available single-particle resonance state, $f_{5/2}$, is the vehicle, whereas the other proton can approach in continuum states of even higher angular momentum. In practice, after tunneling through the barrier into the 2^+ resonance state, in practice only $E2$ electric transition to the ground state is allowed. Background capture through non-resonance continuum states also contributes significantly to the capture process. The sequential 2^+ capture mechanism might for other nuclei be replaced by for example the normally larger 1^- capture.

In conclusion, the two-proton capture rates at a waiting point at the dripline are successfully calculated with a conceptually relatively simple, but technically advanced, new model. The same effective nucleon-nucleon interaction is used for both the nuclear mean-field and the proton-core calculations. The temperature dependent rate and the corresponding capture mechanism are calculated with less ambiguity than in previous calculations. A number of applications are now feasible.

Acknowledgements

This work was funded by the Danish Council for Independent Research DFF Natural Science and the DFF Sapere Aude program. This work has been partially supported by the Spanish Ministerio de Economía y Competitividad under Project FIS2014-51971-P.

References

References

- [1] G. J. Mathews and R. A. Ward, Rep. Prog. Phys. **48**, 1371 (1985).
- [2] A. Barlett *et al.*, Phys. Rev. C **74**, 015802 (2006).
- [3] E.M. Burbidge *et al.*, Rev. Mod. Phys. **29**, 547 (1957).
- [4] M. Arnould and S. Goriely, Phys. Rep. **384**, 1-84 (2003).
- [5] Rauscher T, Dauphas N, Dillmann I, Fröhlich C, Flp Z and Gyrky G, Rep. Prog. Phys. **76**, 066201 (2013).
- [6] R. Reifarh, C. Lederer, Fäppeler, J. Phys. G: Nucl. Part. Phys. **41**, 053101 (2014).
- [7] H. Palme, K. Lodders, A. Jones, *Solar System Abundances of the Elements in Planets, Asteroids, Comets and the Solar System*, A. M. Davis ed., pp 15-36 (2014).
- [8] H. Schatz *et al.*, Phys. Rep. **294**, 167 (1998).
- [9] B.A. Brown, R.R.C. Clement, H.Schatz, and A.Volya, Phys. Rev. C **65**, 045802 (2002).
- [10] S.E. Woosley and W.M. Howard, Astrophys. J. Suppl. **36**, 285 (1978).
- [11] C. Fröhlich, G. Martínez-Pinedo, M. Liebendörfer, F.-K. Thielemann, E. Bravo, W. R. Hix, K. Langanke, and N. T. Zinner, Phys. Rev. Lett. **96**, 142502 (2006).
- [12] C. Fröhlich, P. Hauser, M. Liebendörfer, G. Martnez-Pinedo, *et al.*, Astrophys. J. **637**, 415 (2006)
- [13] M. Oinen *et al.*, Phys. Rev. C **61**, 035801 (2000).
- [14] L.V. Grigorenko and M.V. Zhukov, Phys. Rev. C **72**, 015803 (2005).
- [15] L.V. Grigorenko, R.C. Johnson, I.G. Mukha, I.J. Thompson, and M.V. Zhukov, Phys. Rev. C **64**, 054002 (2001).
- [16] J. Görres, M. Wiescher, and F.-K. Thielemann, Phys. Rev. C **51**, 392 (1995).
- [17] H. Schatz, Int. J. Mass spectrom. **251**, 293 (2006).
- [18] P. Schury *et al.*, Phys. Rev. C **75**, 055801 (2007).
- [19] X.L. Tu *et al.*, Phys. Rev. Lett. **106**, 112501 (2011).
- [20] M. Thoennessen, Rep. Prog. Phys. **67**, 1187 (2004).
- [21] J. Erler *et al.*, Nature **486**, 509 (2012).
- [22] M. Pfitzner, M. Karny, L. V. Grigorenko, and K. Riisager, Rev. Mod. Phys. **84** 567 (2012).
- [23] A.S. Jensen, D.V. Fedorov, and E. Garrido, J. Phys. G: Nucl. Part. Phys. **37**, 064027 (2010).
- [24] E. Garrido, D.V. Fedorov, A.S. Jensen, and H.O.U. Fynbo, Nucl. Phys. A **748**, 27 (2005).
- [25] S. Chekanov *et al.*, Eur. Phys. J. C **51**, 289 (2007).
- [26] R. Álvarez-Rodríguez, H.O.U. Fynbo, A.S. Jensen, and E. Garrido, Phys. Rev. Lett. **100**, 192501 (2008).
- [27] C. Iliadis, *Nuclear physics of stars*, John Wiley & Sons, (2015).
- [28] D. Hove, A. S. Jensen, H. O. U. Fynbo, N. T. Zinner, D. V. Fedorov, and E. Garrido, Phys. Rev. C **93**, 024601 (2016).
- [29] E. Garrido, D.V. Fedorov, and A.S. Jensen, Phys. Rev. C **69**, 024002 (2004).
- [30] D. Hove, E. Garrido, P. Sarriuren, D. V. Fedorov, H. O. U. Fynbo, A. S. Jensen, and N. T. Zinner, Phys. Rev. C **95**, 061301(R) (2017).

- [31] D. Hove, E. Garrido, P. Sarriguren, D.V. Fedorov, H.O.U. Fynbo, A.S. Jensen, and N.T. Zinner, arXiv:1705.08718 (2017)
- [32] D. Hove, E. Garrido, A. S. Jensen, P. Sarriguren, H. O. U. Fynbo, D. V. Fedorov, and N. T. Zinner, Few-Body Syst. **58**, 33 (2017).
- [33] E. Nielsen, D.V. Fedorov, A.S. Jensen, and E. Garrido, Phys. Rep. **347**, 373 (2001).
- [34] A.S. Jensen, K. Riisager, D.V. Fedorov, and E. Garrido, Rev. Mod. Phys. **76**, 215 (2004).
- [35] E. Garrido, Few-body Syst. **56**, 829 (2015).
- [36] R. de Diego, D.V. Fedorov, E. Garrido, and A.S. Jensen, J. Phys. G: Nucl. Part. Phys. **37**, 115105 (2010).
- [37] R. de Diego *et al.*, Phys. Lett. B **695**, 324 (2011).
- [38] R. de Diego, E. Garrido, D.V. Fedorov, and A.S. Jensen, EPL. **90**, 52001 (2010).
- [39] E. Garrido, A.S. Jensen, and D.V. Fedorov, Phys. Rev. C **91**, 054003 (2015).
- [40] E. Garrido, Few-Body Systems **56**, 829 (2015).
- [41] D. Hove *et al.*, Phys. Rev. C **90**, 064311 (2014).
- [42] E. Chabanat, P. Bonche, P. Haensel, J. Meyer, and R. Schaeffer, Nucl. Phys. A **635**, 231 (1998).
- [43] M.D. Santo *et al.*, Phys. Lett. B **738**, 453 (2014).
- [44] M.Wang, G.Audi, A.H.Wapstra, F.G.Kondev, M.MacCormick, X.Xu, and B.Pfeiffer, Chin. Phys. C **36**, 1603 (2012).
- [45] G. Audi *et al.*, Chin. Phys. C **36**, 1287 (2012).
- [46] E. Garrido, R. de Diego, D.V. Fedorov, and A.S. Jensen, Eur. Phys. J. A **47**, 102 (2011).